arXiv:1510.03345v3 [hep-th] 16 Sep 2016

Spectrum Structure of Fermion on Bloch Branes with two Scalar-fermion Couplings

Qun-Ying Xie[a,b]‡, Heng Guo[c], Zhen-Hua Zhao[d], Yun-Zhi Du[e], Yu-Peng Zhang[b]

[a]School of Information Science and Engineering, Lanzhou University, Lanzhou 730000, China
[b]Institute of Theoretical Physics, Lanzhou University, Lanzhou 730000, China
[c]School of Physics and Optoelectronic Engineering, Xidian University, Xi'an 710071, China
[d]Department of Applied Physics, Shandong University of Science and Technology, Qingdao 266590, China
[e]Department of Physics, Shanxi Datong University, Datong 037009, China

Abstract. It is known that the Bloch brane is generated by an odd scalar field ϕ and an even one χ. In order to localize a bulk fermion on the Bloch brane, the coupling between the fermion and scalars should be introduced. However, only the Yukawa coupling between the fermion and the odd scalar ϕ was considered. In this paper, we consider the full coupling between the fermion and the odd and even scalars, and investigate the localization and spectrum structure of the fermion on the Bloch brane. It is found that the full coupling insures that the left-handed fermion zero mode can be localized on the Bloch brane under some conditions, and the effective potentials have richer structure and may be volcano-like, finite square well-like, and infinite potentials. As a result, the spectrum is consisted of a series of resonant Kaluza-Klein fermions, finite or infinite numbers of bound Kaluza-Klein fermions.

‡ E-mail: xieqy@lzu.edu.cn(corresponding author)

1. Introduction

The idea of extra dimensions has received increasing interest since the Arkani-Hamed-Dimopoulos-Dvali (ADD)[1] brane model and Randall-Sundrum (RS) [2, 3] brane model (include RS1 [2] and RS2 [3] models) were presented. Especially, the effective gravity can be still four-dimensional even for the case of the infinite extra dimensions, namely, the extra dimensions are also invisible. This surprised idea was firstly proposed in the RS2 model [3]. The key point is that extra dimensions are warped and hence four-dimensional gravitons are trapped by effective potentials caused by the warped geometry [3]. In the RS2 model, our four-dimensional Universe is a thin brane. The generalizations of the RS2 brane model including thick brane models can be found for examples in Refs. [4, 5, 6, 7, 8, 9]. For the review of thick branes see Ref. [10].

In this paper, our interest is focused on the five-dimensional thick brane models. In these models, one usually introduces one or more background scalar fields that play the role of generating the thick brane [11, 12, 13, 14, 15, 16]. A feature of these models is that the brane may have inner structure. Localization and mass spectra of various bulk matter fields especially fermions on a brane are important and interesting problems [14, 17, 18, 19, 20, 21, 22, 23, 24, 25, 26, 27, 28, 29, 30, 31, 32, 33, 34, 35]. In order to localize fermion zero mode on a brane, one usually needs to introduce Yukawa coupling $\eta\bar{\Psi}F(\phi,\chi,\cdots)\Psi$ [17, 18, 23, 31, 32] between the bulk fermion field Ψ and the background scalar fields ($\phi,\ \chi,\ \cdots$), where $F(\phi,\chi,\cdots)$ is an odd function of these scalars. Under this mechanism, there may exist only one bound massless fermion Kaluza-Klein (KK) mode (the fermion zero mode) [19, 21, 24], or a bound massless KK mode and finite discrete bound massive KK modes (mass gaps) [14, 20]. Furthermore, there also may exist quasi-localized fermion KK modes (also called fermion resonances) on a brane [22, 36, 37].

In Ref. [38], the authors investigated the localization and resonances of fermion on the Bloch brane constructed in Ref. [39]. In the Bloch brane model, there are two real background scalar fields ϕ and χ, which are odd and even functions of the extra dimension, respectively. In order to localize the fermion zero mode on the Bloch brane, the Yukawa coupling $\eta\bar{\Psi}F(\phi,\chi)\Psi$ was introduced [38], where $F(\phi,\chi)=\phi$ is an odd function of the extra dimension. The effective potentials for the left- and right-handed fermion KK modes are volcano-like ones. It was found that the left-handed fermion zero mode is localized on the brane and there are many massive left- and right-handed fermion resonances [38].

However, the Yukawa coupling will do not work if the background scalar fields are even functions of the extra dimension, since the Z_2 reflection symmetry of the effective potentials for the fermion KK modes can not be ensured. Recently, in order to solve this problem, Liu *et al* presented a new localization mechanism with the coupling describing the interaction between π-meson and nucleons in quantum field theory, i.e., $\lambda\bar{\Psi}\Gamma^M\partial_M F(\phi,\chi,\cdots)\gamma^5\Psi$ [40]. This new mechanism has revealed some new interesting results [40, 41, 42]. In the model of a two-scalar-generated brane, the fermion zero mode

is localized on the brane and a mass gap between the fermion zero mode and excited KK modes was found [40]. In another dilaton-scalar-generated brane model, the fermion zero mode can also be localized on the brane but there is no mass gap [40], and fermion resonances may appear [42].

In this paper, we would like to investigate the localization and spectrum structure of a bulk fermion on the Bloch brane by introducing the full coupling between the fermion and the two scalars, including the Yukawa coupling and the new coupling presented in Ref. [40]. It will be found that the effective potentials for the left- and right-handed KK fermions have three typical shapes, i.e., volcano-like, finite square well-like, and infinite potentials, and the spectrum has rich structure. The paper is organized as follows. In Sec. 2, we first give a brief review of the Bloch brane model. Then, in Sec. 3, we study the localization and mass spectrum of fermion on the Bloch brane with only the new scalar-fermion coupling and both the two scalar-fermion couplings. Lastly, a brief discussion and conclusion are presented in Sec. 6.

2. Review of the brane model

Let us review the thick branes that arise from two interactional real scalar fields ϕ and χ with a scalar potential $V(\phi,\chi)$. The five-dimensional action for such a system is

$$S=\int d^5x\sqrt{-g}\Big[\frac{1}{2\kappa_5^2}R-\frac{1}{2}(\partial\phi)^2-\frac{1}{2}(\partial\chi)^2-V(\phi,\chi)\Big], \tag{1}$$

where R is the scalar curvature and we set $\kappa_5^2=2$ in this paper. The line-element for the flat brane system that we are interested in is

$$ds^2=\mathsf{e}^{2A(y)}\eta_{\mu\nu}dx^\mu dx^\nu+dy^2, \tag{2}$$

where y denotes the extra dimension and $\mathsf{e}^{2A(y)}$ is the warp factor. We can get the conformal flat metric

$$ds^2=\mathsf{e}^{2A(z)}\left(\eta_{\mu\nu}dx^\mu dx^\nu+dz^2\right) \tag{3}$$

by using the following coordinate transformation

$$dz=e^{-A(y)}dy. \tag{4}$$

The scalar fields ϕ and χ are functions of y only for the static flat brane, i.e., $\phi=\phi(y)$ and $\chi=\chi(y)$. Substituting the line-element (2) into the five-dimensional action (1), one gets the following second-order nonlinear coupled differential field equations

$$\begin{aligned}
\phi''+4A'\phi' &= \partial_\phi V(\phi,\chi),\\
\chi''+4A'\chi' &= \partial_\chi V(\phi,\chi),\\
12(A')^2+3A'' &= -4V(\phi,\chi),\\
2(\phi'^2+\chi'^2) &= -3V(\phi,\chi).
\end{aligned}$$

where $'$ denotes the derivative with respect to the extra dimension y.

It is not easy to solve the above second-order field equations. However, by introducing an auxiliary superpotential $W=W(\phi,\chi)$ [11, 12, 39, 43, 44], the above

field equations of the Einstein-scalar system can be reduced to the following first-order ones

$$\begin{aligned}\phi' &= \partial_\phi W,\\ \chi' &= \partial_\chi W,\\ 3A' &= -2W.\end{aligned} \tag{5}$$

The corresponding scalar potential V is

$$V = \frac{1}{2}\left[(\partial_\phi W)^2 + (\partial_\chi W)^2\right] - \frac{4}{3}W^2. \tag{6}$$

Following Ref. [45], we also consider the following generalized superpotential

$$W = \phi\left[a\left(v^2 - \frac{1}{3}\phi^2\right) - b\chi^2\right]. \tag{7}$$

Then we can get the explicit expression of the scalar potential $V(\phi,\chi)$. From Ref. [38], we know that there are two minima (two vacua) located at $\chi = 0$ and $\phi = \pm v$ in the scalar potential $V(\phi,\chi)$. For $a = 3b$, there is a very simple brane solution [45]:

$$\begin{aligned}\phi(y) &= v\tanh(ky),\\ \chi(y) &= v\ \mathtt{sech}(ky),\\ A(y) &= \frac{2}{3}v^2\ln \mathtt{sech}(ky),\end{aligned} \tag{8}$$

where $k = 2bv$. For $a = b$, there exists a degenerate Bloch brane solution [45]:

$$\begin{aligned}\phi(y) &= \frac{uv\sinh(ky)}{u\cosh(ky) - c_0},\\ \chi(y) &= \frac{2v}{u\cosh(ky) - c_0},\\ e^{2A(y)} &= \left(\frac{c_0 - u}{c_0 - u\cosh(ky)}\right)^{4v^2/9}\\ &\quad\times\ \exp\left[\frac{4uv^2}{9}\left(\frac{u - c_0\cosh(ky)}{(c_0 - u\cosh(ky))^2} - \frac{1}{u - c_0}\right)\right].\end{aligned} \tag{9}$$

where

$$u = \sqrt{c_0^2 - 4}, \tag{10}$$

and the parameter $c_0 < -2$.

The thickness of the single and double branes could be estimated as

$$\delta \simeq \begin{cases} \frac{1}{bv} & \mathtt{for\ solution}\ (8)\\ \frac{1}{bv}\ln\frac{-2c_0}{\sqrt{c_0^2-4}} & \mathtt{for\ solution}\ (9)\ \mathtt{with}\ c_0 \to -2\end{cases}. \tag{11}$$

The single brane is localized near $z = 0$, while the double branes are localized near $z = \pm\delta/2$ and the thickness of the double brane is δ. In what follows, we mainly discuss the case of the double brane solution (9) (i.e., $c_0 \to -2$ or $u \to 0$). Because when $u \to 0$, a little change to c_0 will lead to a large change of the brane thickness δ, this will add difficulty for us to adjust the brane thickness, then we define a new parameter δ_0

$$\delta_0 = \ln(4/u). \tag{12}$$

Now $u\to 0$ corresponds to $\delta_0 \gg 1$. The thickness of the double brane for solution (9) is

$$\delta \approx \frac{1}{bv}\ln\frac{4}{u} = \frac{\delta_0}{bv}. \tag{13}$$

Thus, the thickness of the brane can be easily adjusted by δ_0, which is an integral parameter independent of the scalar potential $V(\phi,\chi)$.

3. Localization mechanism of a bulk fermion on the Bloch brane

In this section, we would like to investigate the localization of a bulk fermion on the Bloch brane by the two fermion localization mechanisms, one is Yukawa coupling $\eta\bar{\Psi}F_1(\phi,\chi)\Psi$, the other is the new coupling $\lambda\bar{\Psi}\Gamma^M\partial_M F_2(\phi,\chi)\gamma^5\Psi$ [40]. The action is given by

$$\begin{aligned} S_F = \int d^5x\sqrt{-g}\Big(\ & \bar{\Psi}\Gamma^M(\partial_M+\omega_M)\Psi - \eta\bar{\Psi}F_1(\phi,\chi)\Psi \\ & + \lambda\bar{\Psi}\Gamma^M\partial_M F_2(\phi,\chi)\gamma^5\Psi\Big), \end{aligned} \tag{14}$$

where η and λ are the scalar-fermion coupling parameters. With the metric (2), the non-vanishing components of the spin connection ω_M are $\omega_\mu = \frac{1}{2}(\partial_z A)\gamma_\mu\gamma_5$, and the five-dimensional Dirac equation reads as

$$[\gamma^\mu\partial_\mu + \gamma^5\left(\partial_z + 2A'(z)\right) - \eta e^A F_1(\phi,\chi) + \lambda F_2'(\phi,\chi)]\Psi = 0. \tag{15}$$

Next we will study the above five-dimensional Dirac equation. Because of the chiral symmetry of fermions, naturally, we choose the following chiral decomposition of the left- and right-handed fermions:

$$\begin{aligned} \Psi(x,z) &= \sum_n\Big(\psi_{Ln}(x)\hat{f}_{Ln}(z)+\psi_{Rn}(x)\hat{f}_{Rn}(z)\Big) \\ &= \mathsf{e}^{-2A}\sum_n\Big(\psi_{Ln}(x)f_{Ln}(z)+\psi_{Rn}(x)f_{Rn}(z)\Big), \end{aligned} \tag{16}$$

where

$$\hat{f}_{L,R}(z) = \mathsf{e}^{-2A}f_{L,R}(z),\ \ \psi_{Ln,Rn}(x) = \mp\gamma^5\psi_{Ln,Rn}(x).$$

It can be shown that the four-dimensional Dirac fields $\psi_{Ln}(x)$ and $\psi_{Rn}(x)$ satisfy the four-dimensional Dirac equations $\gamma^\mu\partial_\mu\psi_{Ln,Rn}(x) = m_n\psi_{Rn,Ln}(x)$, and the KK modes satisfy the following coupled equations

$$\left[\partial_z + \eta e^A F_1(\phi,\chi) - \lambda\ F_2'(\phi,\chi)\right] f_{Ln}(z) = \ + m_n f_{Rn}(z), \tag{17}$$

$$\left[\partial_z - \eta e^A F_1(\phi,\chi) + \lambda\ F_2'(\phi,\chi)\right] f_{Rn}(z) = \ - m_n f_{Ln}(z). \tag{18}$$

The above coupled equations can be racast into the following Schrödinger-like equations

$$(-\partial_z^2 + V_L(z))f_{Ln} = m_n^2 f_{Ln}, \tag{19}$$

$$(-\partial_z^2 + V_R(z))f_{Rn} = m_n^2 f_{Rn}, \tag{20}$$

where the effective potentials for the left- and right-handed KK modes are determined by [40]

$$V_L(z) = \left(\eta e^A F_1\right)^2 - \eta e^A\left(A'F_1 + F_1'\right) - 2\eta\lambda A F_1 F_2' + \lambda^2\left(F_2'\right)^2 + \lambda\ F_2'', \tag{21}$$

$$V_R(z) = V_L(z)|_{\lambda\to-\lambda,\eta\to-\eta}. \tag{22}$$

In order to obtain the standard four-dimensional action for a massless and a series of massive fermions:

$$S_F = \sum_n \int d^4x \ \bar{\psi}_n(\gamma^\mu \partial_\mu - m_n)\psi_n, \tag{23}$$

the following orthonormality conditions for f_{L_n} and f_{R_n} are needed:

$$\int_{-\infty}^{\infty} f_{Lm} f_{Ln} dz = \delta_{mn} = \int_{-\infty}^{\infty} f_{Rm} f_{Rn} dz, \quad \int_{-\infty}^{\infty} f_{Lm} f_{Rn} dz = 0. \tag{24}$$

From Eqs. (21) and (22), it can be seen that, if there is no coupling, i.e., $\lambda = \eta = 0$, then the effective potentials $V_L(z)$ and $V_R(z)$ will vanish and both the left- and right-handed fermions cannot be localized on the Bloch brane. Since Ref. [38] has already considered the case of Yukawa coupling ($\eta \neq 0$ and $\lambda = 0$), in this paper, we will consider first the new coupling only, i.e., $\eta = 0$ and $\lambda \neq 0$, by taking the simply choice as $F_2(\phi, \chi) = \chi^n$, then we will come to the case of the full coupling.

4. The new coupling

Firstly, we will focus only on the new coupling method by setting $\eta = 0$. Considering the conformal transformation relationship between the physical coordinate y and conformal coordinate z in Eq. (4), the effective potentials $V_{L,R}$ in Eqs. (21) and (22) in the y coordinate turn to

$$V_L(y) = \lambda e^{2A}[\lambda F_2'^2 + A' F_2' + F_2''], \tag{25}$$

$$V_R(y) = V_L|_{\lambda \to -\lambda}, \tag{26}$$

By setting

$$F_2(\phi, \chi) = \chi^n, \tag{27}$$

the explicit forms of the effective potentials (25) and (26) for solution (8) read as

$$V_L(y) = \frac{4}{3} n\lambda b^2 v^{2+n} S^{n+\frac{4v^2}{3}}[-3S^2 + (S^2-1)^2(2v^2 + 3n + 3n\lambda(Sv)^n)], \tag{28}$$

$$V_R(y) = V_L|_{\lambda \to -\lambda}, \tag{29}$$

where $S \equiv \texttt{sech}(ky)$. The values of the effective potentials at $y = 0$ are

$$V_L(0) = -V_R(0) = -4n\lambda b^2 v^{2+n}. \tag{30}$$

In this paper, without loss of generality, we assume $b > 0$ and $v > 0$. The asymptotic behaviors of the effective potentials at $y \to \pm\infty$ for different n are discussed as follows:

- When $n > -\frac{2v^2}{3}$ and $n \neq 0$, the effective potentials trend to vanish at the boundary and one of them is the volcano-like potential. For such potential, there may exist a massless mode and a series of massive resonant fermion modes on the brane.
- When $n = -\frac{2v^2}{3}$, the effective potentials have potential wells and trend to a positive constant $4n^2b^2\lambda^2v^{2+2n}$ when $y \to \pm\infty$, which are finite square well-like potentials. In this case, there may be a localized fermion zero mode and a series of bound massive fermion modes.

- When $n < -\frac{2v^2}{3}$, the asymptotic behavior of the potentials are $V_{L,R}(\pm\infty) \to +\infty$, which will result in infinite bound massive fermion modes on the brane.

  For the solution (9), the effective potentials read as

$$V_L(y) = e^{n\delta_0 - \frac{8}{9}v^2\left(\frac{1}{2+r} - \frac{2+r\cosh(ky)}{(r+2\cosh(ky))^2}\right)} \times \frac{8\lambda n b^2 v^{2+n}(2+r)^{\frac{4v^2}{9}}}{9(r+2\cosh(ky))^{4+n+\frac{4v^2}{9}}}$$
$$\times \Big[\sinh^2(ky)\,\Big(18n\lambda v^n e^{n\delta_0}(r+2\cosh(ky))^{2-n}$$
$$+\, 8v^2(5+3r\cosh(ky)+\cosh(2ky))\Big)$$
$$-\, 9(r+2\cosh(ky))^2\,(2+n+r\cosh(ky)-n\cosh(2ky))\Big], \tag{31}$$
$$V_R(y) = V_L|_{\lambda\to-\lambda}, \tag{32}$$

where $r = \sqrt{4+e^{2\delta_0}}$. From (31) we can see that the values of the effective potentials at $y = 0$ are

$$V_L(0) = -V_R(0) = -8n\lambda b^2 v^{2+n} e^{n\delta_0}\,(2+r)^{-1-n}\,. \tag{33}$$

Similarly, there are also three asymptotic behaviors for the effective potential (31) for different n: $n > -\frac{2v^2}{9}$, $n = -\frac{2v^2}{9}$, and $n < -\frac{2v^2}{9}$ relate to volcano-like, finite square well-like, and infinite potentials, respectively. The asymptotic value of the finite square well-like potentials at the boundary is

$$V_{L,R}(\pm\infty) = \frac{16}{81}\lambda^2 b^2 v^{6-\frac{4v^2}{9}}(2+r)^{\frac{4v^2}{9}} e^{-\frac{4}{9}v^2(\frac{2}{2+r}+\delta_0)} \equiv C_\infty \;>\; 0. \tag{34}$$

In conclusion, the effective potentials have abundant inner structure with different values of n for both brane solutions (8) and (9). The shapes of the effective potentials for the left- and right-handed fermions with different n are shown in Figs. 1 and 2 for the brane solutions (8) and (9), respectively. And Figs. 3 and 4 show how the parameters λ and δ_0 affect the effective potentials: they controls the depth and width of the effective potentials, respectively. For large enough δ_0 the potential V_R will have two wells.

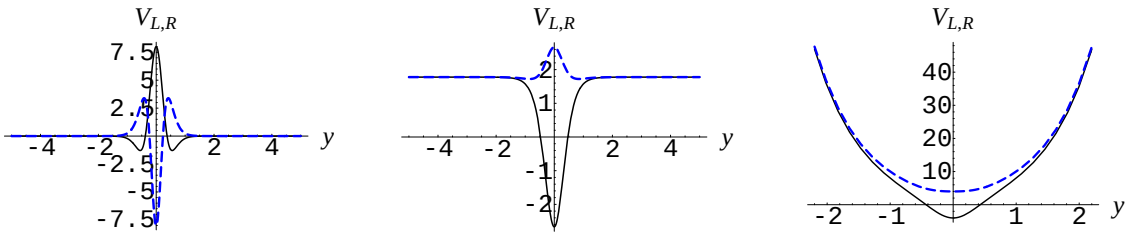

(a) $n = 2$ (b) $n = -\frac{2}{3}$ (c) $n = -1$

Figure 1. Plot of the potentials V_L (black solid line) and V_R (blue dashed line) for the brane solution (8) for different values of n in y coordinate. The parameters are set to $b = 1,\ v = 1,\ \lambda = -1$.

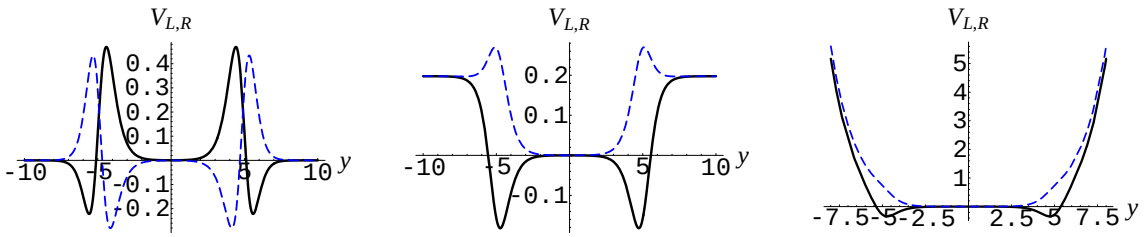

(a) $n = 1$ (b) $n = -\frac{2}{9}$ (c) $n = -0.4$

Figure 2. Plot of the potentials V_L (black solid line) and V_R (blue dashed line) for the brane solution (9) for different values of n in y coordinate. The parameters are set to $b = 1,\ v = 1,\ \lambda = -1,\ \delta_0 = 10$ ($u = 0.00018$).

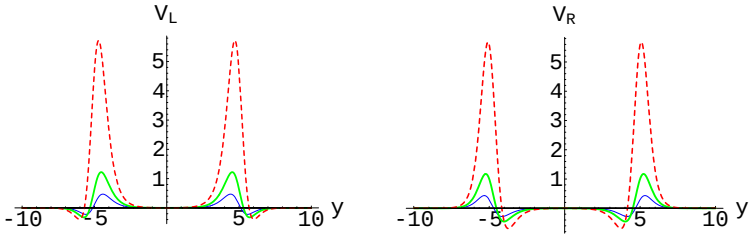

(a) (b)

Figure 3. Plot of the potentials $V_{L,R}$ for the brane solution (9) for different values of λ in y coordinate. The parameters are set to $b = 1,\ v = 1,\ n = 1,\ \delta_0 = 10,\ \lambda = -1$ for blue thin lines, $\lambda = -2$ for green thick lines, and $\lambda = -5$ for the red dashed lines.

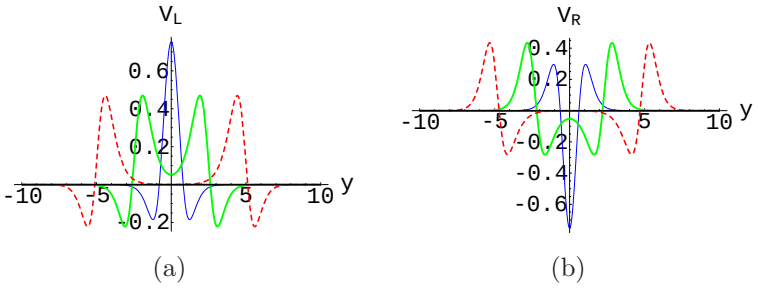

(a) (b)

Figure 4. Plot of the potentials $V_{L,R}$ for the brane solution (9) for different values of δ_0 in y coordinate. The parameters are set to $b = 1,\ v = 1,\ n = 1,\ \lambda = -1,\ \delta_0 = 1$ for blue thin lines, $\delta_0 = 5$ for green thick lines, and $\delta_0 = 10$ for red dashed lines.

4.1. The zero mode

Now, let us investigate the localization of the fermion zero mode under the new coupling mechanism. By setting $m_0 = 0$ and $\eta = 0$ in Eq. (17), we get the solution of the fermion zero modes

$$f_{L0,R0}(z(y)) \propto \exp\left[\pm\lambda\ F_2(\phi,\chi)\right] = \begin{cases} e^{\pm\lambda(v sech(ky))^n} & \texttt{for solution (8)} \\ e^{\pm\lambda\ (\frac{2v}{u\cosh(ky)-c_0})^n} & \texttt{for solution (9)} \end{cases} \quad (35)$$

In order to localize the zero modes on the brane, we need to consider the normalization condition (35):

$$\int dz\ f^2_{L0,R0}(z) \propto \int dz\ e^{\pm 2\lambda F_2(\phi,\chi)} < \infty, \tag{36}$$

which indicates that only one of the left- and right-handed fermion zero modes may be localized on the brane. Since we do not have the analytic expressions of the functions $A(z)$ and $\chi(z)$ in the z coordinate, we have to deal with them in the y coordinate. With the relation (4) between y and z, the normalization condition of the left-handed fermion zero mode is turned out to be

$$\int_{-\infty}^{\infty} dy\ e^{2\lambda(v sech(ky))^n - A(y)} < \infty \quad \texttt{for solution}\ (8), \tag{37}$$

$$\int_{-\infty}^{\infty} dy\ e^{2\lambda(\frac{2v}{u\cosh(ky)-c_0})^n - A(y)} < \infty\ \texttt{for solution}\ (9). \tag{38}$$

Since we have let $b > 0$ and $v > 0$, the normalization condition in (38) is

$$n < 0\ \ \texttt{and}\ \ \lambda < 0,\ \ \texttt{for solution}\ (8). \tag{39}$$

With the solution (9) for $A(y)$, we can get the explicit expression of the integrand in (38):

$$\begin{aligned} \texttt{EI} = \Big(\ \frac{c_0 - u}{c_0 - u\cosh(ky)}\Big)^{\frac{-2v^2}{9}} \times \exp\Big[2\lambda(\frac{2v}{u\cosh(ky) - c_0})^n \\ - \frac{2uv^2}{9}\Big(\frac{u - c_0\cosh(ky)}{(c_0 - u\cosh(ky))^2} - \frac{1}{u - c_0}\Big)\Big]. \end{aligned} \tag{40}$$

Since $u > 0$, $v > 0$, $c_0 < -2$, the asymptotic behavior of EI at $y \to \pm\infty$ is

$$\texttt{EI} \to \begin{cases} +\infty & \texttt{for}\ n > 0, \\ +\infty & \texttt{for}\ n < 0\ \texttt{and}\ \lambda > 0, \\ 0 & \texttt{for}\ n < 0\ \texttt{and}\ \lambda < 0. \end{cases} \tag{41}$$

Figure 5 shows the left-handed fermion zero mode f_{L0} and the integrand EI with different parameters n and δ. It is not difficult to see that the integrand EI in (40) is convergent when $n < 0$ and $\lambda < 0$. So the normalization condition for the left-handed fermion zero mode is

$$n < 0\ \ \texttt{and}\ \ \lambda < 0,\ \ \texttt{for solution}\ (9). \tag{42}$$

Under the conditions (39) and (42) for solutions (8) and (9), respectively, the left-handed fermion zero mode can be localized on the brane. This result is consistent with Fig. 5.

4.2. Volcano-like potentials and massive resonant KK modes

Next, we would like to investigate the massive fermion KK modes. We will consider three kinds of effective potentials mentioned before respectively. This subsection deals with the volcano-like potentials, for which the massive KK modes can propagate along the extra dimension and there may be some quasi-localized or resonant fermion KK

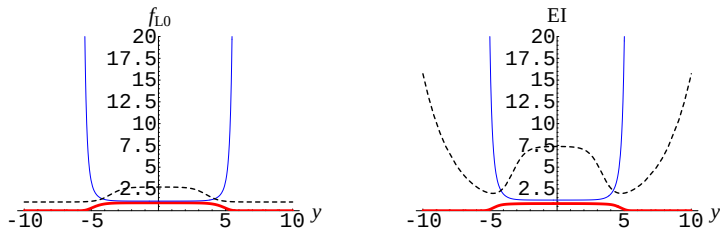

(a) (b)

Figure 5. Plot of the left-handed fermion zero mode f_{L0} and the integrand EI (40) for the brane solution (9). The parameters are set to $b = 1,\ v = 1,\ k = 2,\ u = 0.002$. Other parameters are set to $n = -1, \lambda = -0.1$ for red thick lines, $n = -1, \lambda = 0.1$ for blue thin lines, and $n = 1, \lambda = 1$ for the dashed lines.

modes localized on the brane for finite time [22, 37]. We will take our focus on the study of these special KK modes.

The study of resonant fermion on thick branes [12, 22, 27, 46, 47, 48, 49] is rich and interesting. In Ref. [22], the resonant fermion problem on the Bloch brane model has been studied with the Yukawa coupling. By comparing the value of the wave-function at the origin, i.e., $|R(0)|$, to the amplitude of the plane wave oscillations at large distance along extra dimension, the authors of Ref. [22] have investigated the even massive fermionic resonant modes.

In Refs. [38, 50], the relative probability [37] and transmission coefficient [51, 52, 53] methods were used to find fermion KK resonances. The conclusion is that the two methods are consistent with each other. In this paper, we would like to use the relative probability method.

One can define $|f(z)|^2$ as the probability for finding a massive fermion KK mode at the position z along extra dimension. Within a narrow range $-z_b \leq z \leq z_b$ around the brane location, the relative probability named P is defined in a box with borders $|z| = 10z_b$ as follows [37]:

$$P(m) = \frac{\int_{-z_b}^{z_b} |f(z)|^2 dz}{\int_{-10z_b}^{10z_b} |f(z)|^2 dz}. \tag{43}$$

Note that when the mass square m^2 is much larger than the maxima of the effective potentials $V_{L,R}^{max}$, i.e., $m^2 \gg V_{L,R}^{max}$, the KK mode $f(z)$ can be approximated as a plane wave function $f(z) \propto \cos mz$ or $\sin mz$, and the corresponding probability would trend to 0.1.

It is known from the previous subsection that only one of the left- and right-handed fermion zero modes can be localized on the brane. In order to obtain the localized left-handed fermion zero mode, conditions (39) and (42) should be satisfied. So we only consider the case of $\lambda < 0$ and $n < 0$.

For the set of parameters $b = 1, v = 3,\ n = -1, \delta_0 = 25$ and $\lambda = -2$, we get four resonances with mass spectrum $m^2 = \{0.5612, 1.2386, 2.1677, 3.3594\}$ for both left- and

right-handed fermions. Figure 6(a) shows the resonance spectrum of the right-handed fermions.

Next we consider the same set of parameters but with double coupling constant λ, i.e., $\lambda = -4$. It is found that there are eight fermion resonances (see Fig. 6(b)), and the mass spectrum of the resonances is calculated as

$$m^2 = \{0.9319, 1.4071, 2.4778, 3.8263, 5.4279, 7.2663, 9.307, 11.5921\}. \quad (44)$$

For the third set of parameters $b = 1, v = 3,\ n = -1, \delta_0 = 50$ and $\lambda = -2$, i.e., the case with double width δ_0 compared to the first set of parameters, we find ten fermion resonances (see Fig. 6(c)), and the mass spectrum of the resonances is

$$m^2 = \{0.1414, 0.3173, 0.5617, 0.8733, 1.2509, \\ 1.6954, 2.205, 2.7863, 3.4289, 4.1523\}. \quad (45)$$

These results and further calculations show that the number of the resonant fermions increases with the absolute value of the coupling parameter λ and the brane width $\delta = \delta_0/(bv)$.

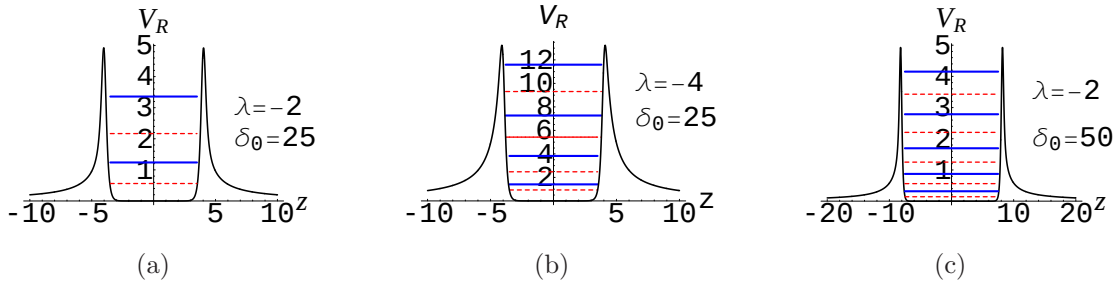

Figure 6. The effective potential $V_R(z)$ and the resonance spectrum m_n^2 of the right-handed fermion for the brane solution (9). m_n^2 for odd and even resonance KK modes are denoted by the red dashed and blue solid lines, respectively. The parameters are set to $b = 1,\ v = 3,\ n = -1$, λ and δ_0 are shown in the figures.

4.3. Finite square well-like potentials and massive bound KK modes

When the parameter n is taken as the special value $n = -\frac{2v^2}{9}$ for the brane solution (9), the effective potential (31) will change to the finite square well-like shape, for which there will appear some bound KK modes. Next, we will search for the bound states and investigate the effect of the parameters λ and δ_0 to the bound KK modes.

For $b = v = 1,\ \beta = 0,\ n = -2/9,\ \delta_0 = 1$ and $\lambda = -10$, we find five massive bound states for both the left and right-handed fermions, and the same mass spectrum of the massive bound states reads

$$m^2 = \{6.9527, 12.3648, 16.238, 18.7367, 20.1259\}. \quad (46)$$

The finite square well-like potentials $V_{L,R}$ and the corresponding first several wave functions of the bound states are shown in Figs. 7 and 8, respectively. Compare Fig. 7

with Fig. 8, one can get the conclusion that except for the zero mode of the left-handed fermion, both of the massive bound states for the left and right-handed fermions are the same.

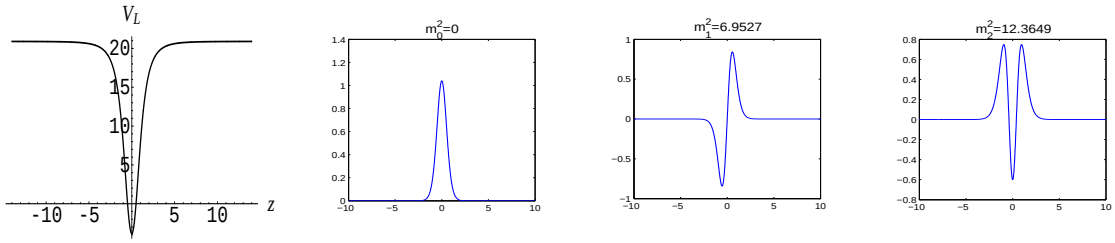

(a) V_L (b) f_{L0} (c) f_{L1} (d) f_{L2}

Figure 7. Plot of the potential V_L and the wave functions of the first three bound states f_{Ln} with square of mass m_n^2 for the brane solution (9). The parameters are set to $b = 1,\ v = 1,\ n = -2/9,\ \delta_0 = 1, \lambda = -10$.

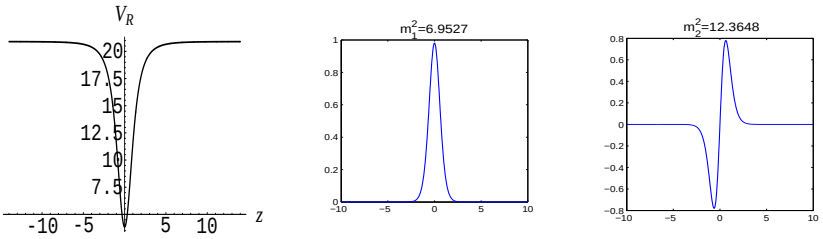

(a) V_R (b) f_{R1} (c) f_{R2}

Figure 8. Plot of the potential V_R and the wave functions of the first two bound states f_{Rn} with square of mass m_n^2 for the brane solution (9). The parameters are set to $b = 1,\ v = 1,\ n = -2/9,\ \delta_0 = 1, \lambda = -10$.

When double the value of the parameter δ_0, i.e., $b = v = 1,\ \beta = 0,\ n = -2/9,\ \delta_0 = 2$ and $\lambda = -10$, which will cause the double width of the potential than the last set of parameters, we find five massive bound states for both the left and right-handed fermions, and the mass spectrum of the massive bound states is listed as

$$m^2 = \{4.2592, 8.7203, 12.6784, 15.8185, 18.0067\}. \tag{47}$$

For $b = v = 1,\ \beta = 0,\ n = -2/9,\ \delta_0 = 1$ and $\lambda = -20$, double the depth of the potentials than that of the first set of parameters, we find nine bound states for the right-handed fermions, and the mass spectrum is

$$\begin{aligned} m^2 = \{&14.6672, 27.8297, 39.4216, 49.4349, \\ &57.9047, 64.9008, 70.5203, 74.8873, 78.1447\}. \end{aligned} \tag{48}$$

It is interesting to note that there will appear double-well shape of effective potentials with the increase of the width of the well, i.e, parameters δ_0. So, is there any

difference between the bound states of the single- and double-well effective potentials? Next, we will find the bound states for the double-well potentials.

For $b = 1,\ v = 3,\ \beta = 0,\ n = -2, \delta_0 = 25$, and $\lambda = -1$, we find four bound massive states for the left-handed fermions, and the mass spectrum is calculated as

$$m^2 = \{0.12821, 0.50687, 1.1148, 1.8859\}. \tag{49}$$

For the same set of parameters for the double-well potential, we find four bound states for the right-handed fermions, and the mass spectrum is given by

$$m^2 = \{0.12817, 0.50683, 1.1148, 1.8858\}. \tag{50}$$

It can be seen that except for the left-handed zero mode, both the mass spectra for the left- and right-handed fermions are the same. This is same as the case of the single-well brane.

When double the value of the parameter λ, i.e., $b = 1,\ v = 3,\ \beta = 0,\ n = -2,\ \delta_0 = 25$ and $\lambda = -2$, we find seven massive bound states for both the left and right-handed fermions, with the mass spectrum given by

$$m^2 = \{0.1452, 0.5776, 1.2892, 2.2665, 3.4900, 4.9292, 6.5265\}. \tag{51}$$

We come to the conclusion that, except for the fermion zero mode, the mass spectra of the massive bound states for both the left- and right-handed fermions are the same. Besides, the number of the bound fermion KK modes increases with the scalar-fermion coupling parameter λ and the brane width parameter δ_0. Therefore, the double-well potentials will trap more bound KK fermions than single-well ones.

For the infinite square well-like potentials, there exist infinite bound states. We will not discuss them here any more.

5. The full coupling

Since the Bloch brane is generated by two real scalar fields, we should take into account both the Yukawa (for the odd function ϕ) and new (for the even function χ) couplings for the localization and spectrum structure of a bulk fermion on this brane. In this subsection, we will analyze this issue.

The explicit potentials $V_{L,R}$ with the two couplings can be calculated directly according to Eqs. (21) and (22), but we do not show them here. We just analyze the asymptotic behavior of the potentials and the localization condition for the left-handed fermion zero mode.

The values of the potentials for the left and right-handed fermions at $y = 0$ are given by

$$V_L(0) = -V_R(0) = \frac{2ubv^2}{c_0 - u}\eta - \frac{8n\ 4^n b^2 v^{2+n}}{u^n(2+r)^{1+n}}\lambda, \tag{52}$$

where $c_0 \to -2$ and $u = 4e^{-\delta_0}$.

Next, we will analyze the asymptotic behavior of the effective potentials with the full coupling. They have voalno-like shapes if only the Yukawa coupling are considered

($\eta \neq 0,\ \lambda = 0$). So, it is not difficult to see that there are three typical shapes for the full coupling with nonvanishing η and λ. The corresponding asymptotic behaviors are

$$V_{L,R}(y \to \pm\infty) \to \begin{cases} 0 & \texttt{for } n > -\frac{2v^2}{9} \\ C_\infty & \texttt{for } n = -\frac{2v^2}{9} \\ +\infty & \texttt{for } n < -\frac{2v^2}{9} \end{cases}, \tag{53}$$

where C_∞ is a positive constant given in Eq. (34). The typical shapes of the effective potential V_L for only Yukawa coupling, only new coupling, and the full coupling are shown in Fig. 9.

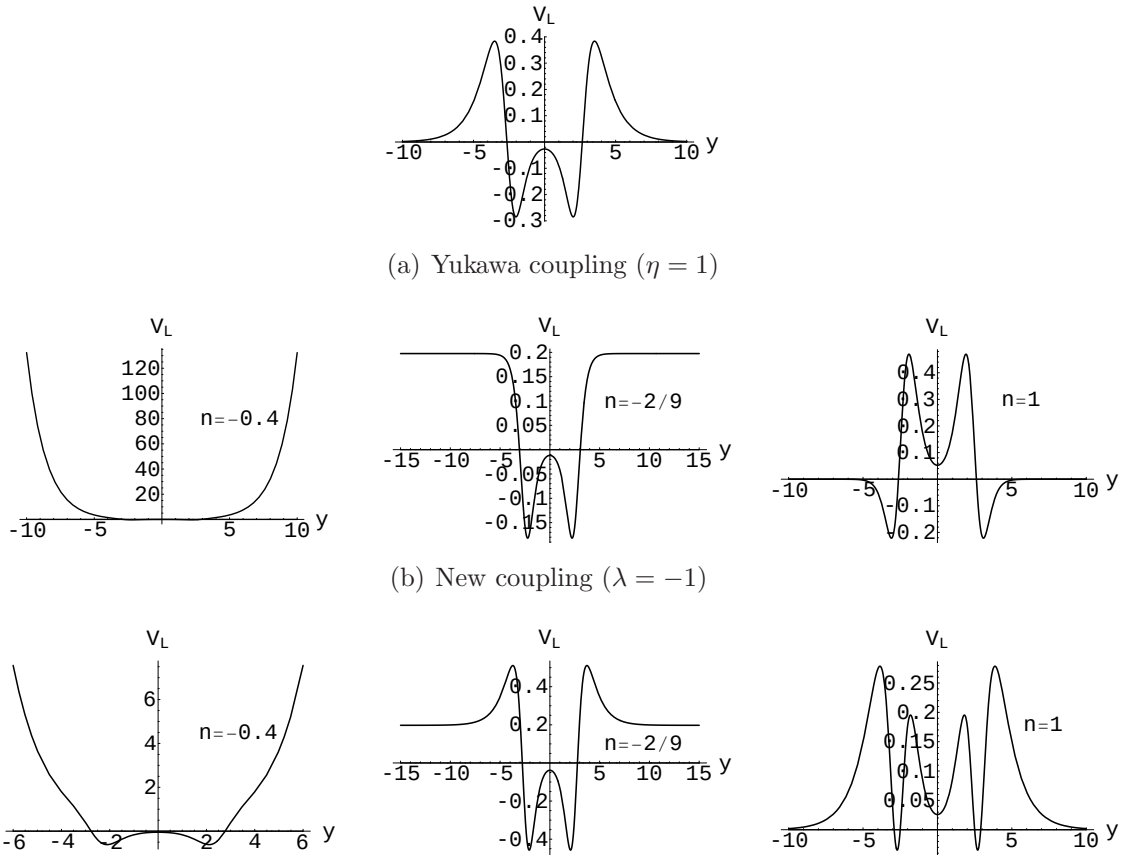

(a) Yukawa coupling ($\eta = 1$)

(b) New coupling ($\lambda = -1$)

(c) Full coupling ($\eta = 1,\ \lambda = -1$)

Figure 9. The effective potential V_L for only Yukawa coupling, only new coupling, and the full coupling. The parameters are set as $b = 1, v = 1, \delta = 5$.

5.1. The zero mode

By setting $m_0 = 0$ in Eq. (17), we get the zero mode $f_{L0}(y)$ for the full coupling:

$$\begin{aligned} f_{L0}(y) &\propto \exp\left[\lambda\ F_2(\phi,\chi) - \eta \int_0^z e^{A(z')} F_1(\phi,\chi) dz'\right] \\ &\propto \exp\left[\lambda\ \chi^n - \eta \int_0^z e^{A(z')} \phi\ dz'\right] \end{aligned}$$

$$\propto \exp\left[\lambda\ \chi^n(y) - \eta \int_0^y \phi(y')\ dy'\right]. \tag{54}$$

The normalization condition for this zero mode is

$$\int_{-\infty}^{+\infty} dy \exp\Big(2\lambda\chi^n - A(y) - 2\eta \int_0^y dy'\phi(y')\Big) < \infty. \tag{55}$$

The integrand in Eq. (55) can be expressed as

$$\begin{aligned}\mathtt{EI_F} \propto\ & \exp\Big[2\lambda\Big(\frac{2v}{u\cosh(ky) - c_0}\Big)^n - \frac{2uv^2(u - c_0\cosh(ky))}{9(u\cosh(ky) - c_0)^2} \\ & + \Big(\frac{2v^2}{9} - \frac{\eta}{b}\Big)\ln\left(u\cosh(ky) - c_0\right)\Big].\end{aligned} \tag{56}$$

The asymptotic behavior of $\mathtt{EI_F}$ at $y \to \pm\infty$ is

$$\mathtt{EI_F}(y \to \pm\infty) \to \begin{cases} e^{(\frac{2v^2}{9} - \frac{\eta}{b})k|y|} & \text{for } n > 0 \\ e^{2^{2n+1}\left(\frac{v}{u}\right)^n \lambda e^{-nk|y|}} & \text{for } n < 0 \end{cases}. \tag{57}$$

So, the normalization condition is $\eta > \frac{2bv^2}{9}$ and $\lambda < 0$ for $n > 0$ and $n < 0$, respectively. It is interesting to note that the normalization condition is related to not only the coupling constant η or λ but also the parameter n.

The zero mode (54) in the y coordinate can be explicitly written as

$$f_L(y) \propto [u\cosh(ky) - c_0]^{-\frac{\eta}{2b}} e^{\lambda(\frac{2v}{u\cosh(ky) - c_0})^n}, \tag{58}$$

from which one can see that it is localized near the Bloch brane and is the ground state. Hence there is no tachyon spectrum for the KK fermions with the full coupling.

5.2. The massive resonant and bound KK modes

At last, we discuss the massive resonant and bound KK modes for the full coupling.

For the case of infinite potential (see the first figure in Fig. 9(c)), there exists infinite bound KK modes. For the case of triple-well potential (see the third figure in Fig. 9(c)), one can obtain some resonant KK modes. We do not go further for these two situations. We will analyze the particular case shown in the second figure in Fig. 9(c).

For the set of parameters given in Fig. 9(c), we find only bound KK modes but no resonant ones for the second potential. The reason is that the potential barrier is not high enough. In order to compare to the case of new coupling only shown in Fig. (7) with six bound KK modes, we set also $b = v = 1,\ n = -2/9,\ \delta_0 = 1,\ \lambda = -10$, but $\eta = 10$. The results are shown in Fig. (10), i.e., besides the zero mode, there are one massive bound KK mode with $m^2 = 15.2356$ and two massive resonant KK modes with $m^2 = 29.9429$ and 42.1322. It is clear that the number of the bound KK mode decreases but the resonances emerge. This is because the appearance of the potential barrier and the narrowing of the potential well. Surely, we will get less bound modes but more resonant modes with the increase of the coupling constant η.

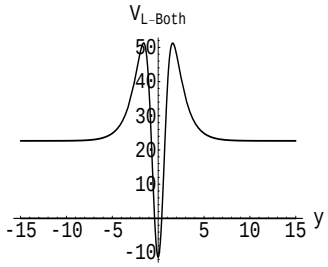

(a) Effective potential

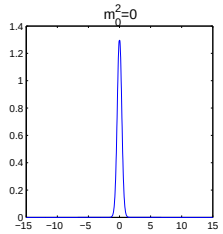

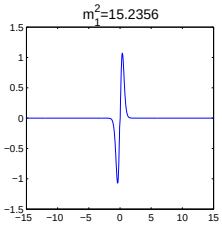

(b) Bound KK modes

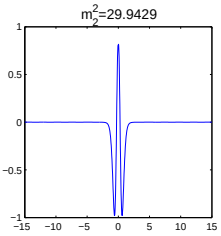

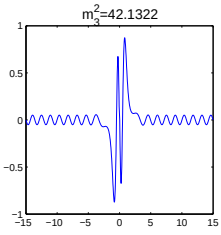

(c) Resonant KK modes

Figure 10. The effective potential V_L and corresponding bound and resonant KK modes for the full coupling. The parameters are set to $b = v = 1,\ n = -2/9,\ \delta_0 = 1,$ $\lambda = -10,\ \ \eta = 10.$

6. Discussions and conclusions

In this paper we have investigated the localization and spectrum structure of a bulk fermion on the Bloch brane. There are two background scalar fields in this brane model, an odd ϕ and an even χ. Therefore, we considered the full coupling between the fermion and the two scalar fields, including the Yukawa coupling $-\eta\bar{\Psi}F_1(\phi,\chi)\Psi$ and the new coupling $\lambda\bar{\Psi}\Gamma^M\partial_M F_2(\phi,\chi)\gamma^5\Psi$. The left-handed fermion zero mode and its localization condition are obtained. If we only consider the Yukawa coupling with $F_1 = \phi$, the effective potential V_L for the left-handed KK modes is volcano-like and there are some resonant KK modes [38]. For the case of the new coupling with $F_2 = \chi^n$, the effective potential V_L has three types of shapes: volcano-like, finite square well-like, and infinite potentials. Correspondingly, there may appear finite numbers of resonant KK fermions, finite and infinite bound KK fermions. The number of the resonant or bound KK fermions increases with the scalar-fermion coupling parameter λ and the brane width parameter δ_0. The similar results were obtained for the full coupling except for the case of $n = -2v^2/9$, for which the effective potential V_L has not only well but also barrier, and subsequently both massive bound and resonant modes appear in the spectrum.

7. Acknowledgement

This work was supported by the National Natural Science Foundation of China (Grants No. 11375075 and No. 11522541), and the Fundamental Research Funds for the Central

Universities (Grant No. lzujbky-2015-107 and No. lzujbky-2016-k04). H. Guo was supported by the National Natural Science Foundation of China (Grants No. 11305119). Z.-H. Zhao was supported by the National Natural Science Foundation of China (Grant No. 11305095).

[1] N. Arkani-Hamed, S. Dimopoulos, and G.R. Dvali, Phys. Lett. **B 429** (1998) 263, arXiv:hep-ph/9803315.
[2] L. Randall and R. Sundrum, Phys. Rev. Lett. **83** (1999) 3370, arXiv:hep-ph/9905221.
[3] L. Randall and R. Sundrum, Phys. Rev. Lett. **83** (1999) 4690, arXiv:hep-th/9906064.
[4] T. Gherghetta and A. Kehagias, Phys. Rev. Lett. **90** (2003) 101601, arXiv:hep-th/0211019.
[5] I. Antoniadis, A. Arvanitaki, S. Dimopoulos, and A. Giveon, Phys. Rev. Lett. **108** (2012) 081602, arXiv:1102.4043[hep-ph].
[6] F.-W. Chen, Y. Zhong, Y.-Q. Wang, S.-F. Wu, and Y.-X. Liu, Phys. Rev. **D 88** (2013) 104033, arXiv:1201.5922[hep-th].
[7] K. Yang, Y.-X. Liu, Y. Zhong, X.-L. Du, and S.-W. Wei, Phys. Rev. **D 86** (2012) 127502, arXiv:1212.2735[hep-th].
[8] B. Guo, Y.-X. Liu, and K. Yang, Eur. Phys. J. **C 75** (2015) 63, arXiv:1405.0074[hep-th].
[9] A. de Souza Dutra, G.P. de Brito, and J.M. Hoff da Silva, Phys. Rev. **D 91** (2015) 086016, arXiv:1412.5543[hep-th].
[10] V. Dzhunushaliev, V. Folomeev, and M. Minamitsuji, Rept. Prog. Phys. **73** (2010) 066901, arXiv:0904.1775[gr-qc].
[11] O. DeWolfe, D.Z. Freedman, S.S. Gubser, and A. Karch, Phys. Rev. **D 62** (2000) 046008, arXiv:hep-th/9909134.
[12] M. Gremm, Phys. Lett. **B 478** (2000) 434, arXiv:hep-th/9912060.
[13] C. Csaki, J. Erlich, T. Hollowood, and Y. Shirman, Nucl. Phys. **B 581** (2000) 309, arXiv:hep-th/0001033.
[14] N. Barbosa-Cendejas, A. Herrera-Aguilar, M. A. ReyesSantos, and C. Schubert, Phys. Rev. **D 77** (2008) 126013, arXiv:0709.3552[hep-th].
[15] Y.-X. Liu, Y. Zhong, and K. Yang, Europhys. Lett. **90** (2010) 51001, arXiv:0907.1952[hep-th].
[16] D. Bazeia, F.A. Brito, and F.G. Costa, Phys. Rev. **D 87** (2013) 065007, arXiv:1210.6318[hep-th].
[17] S. Randjbar-Daemi and M. Shaposhnikov, Phys. Lett. **B 492** (2000) 361, arXiv:hep-th/0008079.
[18] T.R. Slatyer and R.R. Volkas, JHEP **0704** (2007) 062, arXiv:hep-ph/0609003.
[19] Y.-X. Liu, X.-H. Zhang, L.-D. Zhang, and Y.-S. Duan, JHEP **0802** (2008) 067, arXiv:0708.0065[hep-th].
[20] Y.-X. Liu, L.-D. Zhang, S.-W. Wei, and Y.-S. Duan, JHEP **0808** (2008) 041, arXiv:0803.0098[hep-th].
[21] D. Bazeia, F.A. Brito, and R.C. Fonseca, Eur. Phys. J. **C 63** (2009) 163, arXiv:0809.3048[hep-th].
[22] C. A. S. Almeida, R. Casana, M. M. Ferreira Jr., and A. R. Gomes, Phys. Rev. **D 79** (2009) 125022, arXiv:0901.3543[hep-th].
[23] L.B. Castro, Phys.Rev. **D 83** (2011) 045002, arXiv:1008.3665[hep-th].
[24] C.-E. Fu, Y.-X. Liu, and H. Guo, Phys. Rev. **D 84** (2011) 044036, arXiv:1101.0336[hep-th].
[25] A.E.R. Chumbes, A.E.O. Vasquez, and M.B. Hott, Phys. Rev. **D 83** (2011) 105010, arXiv:1012.1480[hep-th].
[26] Y.-X. Liu, X.-N. Zhou, K. Yang, and F.-W. Chen, Phys. Rev. **D 86** (2012) 064012, arXiv:1107.2506[hep-th].
[27] M. Gogberashvili, P. Midodashvili, and L. Midodashvili, Int. J. Mod. Phys. **D 21** (2012) 1250081, arXiv:1209.3815[hep-th].
[28] H. Christiansen and M. Cunha, Eur. Phys. J. **C 72** (2012) 1942, arXiv:1203.2172[hep-th].
[29] W.T. Cruz, A.R.P. Lima, and C.A.S. Almeida, Phys. Rev. **D 87** (2013) 045018, arXiv:1211.7355[hep-th].
[30] W.T. Cruz, R.V. Maluf, and C.A.S. Almeida, Eur. Phys. J. **C 73** (2013) 2523, arXiv:1303.1096[hep-th].

[31] N. Barbosa-Cendejas, D. Malagn-Morejn, and R. Rigel Mora-Luna, Gen.Rel.Grav. **47** (2015) 7, arXiv:1503.07900[hep-th].
[32] G. Alencar, R.R. Landim, M.O. Tahim, and R.N. Costa Filho, Phys.Lett. **B 739** (2014) 125, arXiv:1409.4396[hep-th].
[33] Carlos A. Vaquera-Araujo, Olindo Corradini, Eur.Phys.J. **C 75** (2015) 48, arXiv:1406.2892[hep-th].
[34] V.K. Oikonomou, Class.Quant.Grav. **31** (2014) 025018, arXiv:1308.2085[hep-th].
[35] P. Jones, G. Munoz, D. Singleton, and Triyanta, Phys.Rev. **D 88** (2013) 025048, arXiv:1307.3599[hep-th].
[36] Y.-X. Liu, C.-E. Fu, L. Zhao, and Y.-S. Duan, Phys. Rev. **D 80** (2009) 065020, arXiv:0907.0910[hep-th].
[37] Y.-X. Liu, J. Yang, Z.-H. Zhao, C.-E. Fu, and Y.-S. Duan, Phys. Rev. **D 80** (2009) 065019, arXiv:0904.1785[hep-th].
[38] Q.-Y. Xie, J. Yang, and L. Zhao, Phys. Rev. **D 88** (2013) 105014, arXiv:1310.4585[hep-th].
[39] D. Bazeia and A.R. Gomes, JHEP **0405** (2004) 012, arXiv:hep-th/0403141.
[40] Y.-X. Liu, Z.-G. Xu, F.-W. Chen, and S.-W. Wei, Phys. Rev. **D 89** (2014) 086001, arXiv:1312.4145[hep-th].
[41] Q.-Y. Xie, Z.-H. Zhao, Y. Zhong, J. Yang, and X.-N. Zhou, JCAP **1503** (2015) 014, arXiv:1410.5911[hep-th].
[42] H. Guo, Q.-Y. Xie, and C.-E. Fu, Phys. Rev. **D 92** (2015) 106007, arXiv:1408.6155[hep-th].
[43] V.I. Afonso, D. Bazeia, and L. Losano, Phys. Lett. **B 634** (2006) 526, arXiv:hep-th/0601069.
[44] A. de Souza Dutra, Phys. Lett. **B 626** (2005) 249. arXiv:0705.2903[hep-th].
[45] A. de Souza Dutra, A.C. Amaro de Faria Jr., and M. Hott, Phys. Rev. **D 78** (2008) 043526, arXiv:0807.0586[hep-th].
[46] M. Cvetic and M. Robnik, Phys. Rev. **D 77** (2008) 124003, arXiv:0801.0801[hep-th].
[47] C. Csaki, J. Erlich, T. J. Hollowood, and Y. Shirman, Nucl. Phys. **B 581** (2000) 309, arXiv:hep-th/0001033.
[48] D. Bazeia, A. Gomes, and L. Losano, Int. J. Mod. Phys. **A 24** (2009) 1135, arXiv:0708.3530[hep-th].
[49] J. Hoff da Silva and R. da Rocha, Europhys. Lett. **100** (2012) 11001, arXiv:1209.0989[hep-th].
[50] Y.-Z. Du, L. Zhao, Y. Zhong, C.-E. Fu, and H. Guo, Phys. Rev. **D 88** (2013) 024009, arXiv:1301.3204[hep-th].
[51] R. Landim, G. Alencar, M. Tahim, and R. Costa Filho, JHEP **1108** (2011) 071, arXiv:1105.5573[hep-th].
[52] R. Landim, G. Alencar, M. Tahim, and R. Costa Filho, JHEP **1202** (2012) 073, arXiv:1110.5855[hep-th].
[53] G. Alencar, R. Landim, M. Tahim, and R. C. Filho, JHEP **1301** (2013) 050, arXiv:1207.3054[hep-th].